Hole motion in quantum antiferromagnets: String and hopping results

W. G. Macready and A. E. Jacobs
Department of Physics, University of Toronto, Toronto, Ontario, Canada M5S 1A7
(Received 3 January 1991; revised manuscript received 9 April 1991)

We have investigated the t-J model and its variants using the string basis (of Shraiman, Siggia, Emery, and Lin) and the hopping basis (of Trugman); both bases are generated by the hopping term in the Hamiltonian applied repeatedly to the Néel state with a single hole. For the string basis, states to order t^{10} are treated exactly, so that the Green function is obtained to order t^{20}; the tree approximation (of Brinkman and Rice) is used for the remainder. The hopping basis, which relaxes constraints imposed in the string basis, contains all states generated by up to eight hops. Properties studied include the wave function, the ground-state energy, the effective mass, the bandwidth, the spectral function, the self-energy, and the density of states. For the $U = \infty$ model, there are no quasiparticles; the ferromagnetic polaron is missed. For the t-J_z model, both the string and hopping bases provide excellent results for $J_z > 0.1t$. The Ising limit of the t-J model is treated well by the string basis, but the Heisenberg limit $J_\perp = J_z$ requires the hopping basis, which gives apparently good results for all $J > 0.1t$. The mass is highly anisotropic; for example, at J=0.4t the masses parallel and perpendicular to the magnetic zone face are $m_\parallel = 20.4m$ and $m_\perp = 2.1m$.

I. INTRODUCTION

The high-temperature superconductors now number over a dozen compounds, all containing the Cu-O_2 planes of the original material.[1] Anderson has maintained from the beginning,[2] and has recently argued forcefully,[3] that these are highly correlated systems whose understanding requires the solution of the two-dimensional, single-band Hubbard model:[4] "We must solve the old problem of doping a single Mott-Hubbard band before we can *begin* the problem of high T_c." The transition from antiferromagnetic insulator to superconductor on doping the parent compounds La_2CuO_4 and $YBa_2Cu_3O_6$, and the observation of short-range antiferromagnetic order in superconducting material above its transition temperature[5] are certainly not at variance with this approach.

The Hubbard model has been studied for many years; recent attention has focused on its large-U limit, the t-J model, which reduces to the antiferromagnetic, spin-$\frac{1}{2}$ Heisenberg model at half filling. The ground state of the latter has been established by many workers (conclusively by Liang[6]) to be a Néel state (with the staggered magnetization reduced to about 60% of the classical value by quantum fluctuations); numerical techniques and results are reviewed by Barnes.[7] The Néel state is then a natural starting point for a numerical investigation of hole motion.

The string of bad bonds generated by hole motion in an antiferromagnet figures prominently in many papers; perhaps the earliest treatment is by Bulaevskii *et al.*,[8] who argued that the hole is trapped in a linear potential (in the continuum limit). Brinkman and Rice[9] considered the $J = 0$ limit, and summed the retracing paths to all orders. The string basis was proposed by Shraiman and Siggia[10] (who treated the case of nonzero J), and an analytical Lanczos procedure for generating the basis was devised by Emery and Lin;[11] the basis has been used also in other papers.[12,13] In an important advance, Trugman[14] showed that certain paths in a Néel antiferromagnet displace the hole (by $\sqrt{2}a$ or $2a$) to sites on the same sublattice, leaving the Néel background undisturbed; that is, the hole is not trapped (but it must pass through a barrier[14,15]). The string idea is used in a diagrammatic approach,[15] and it can be extended to two-hole states[10] to examine the possible binding of a pair of holes.[16] Closely related to the string basis is the hopping basis suggested by Trugman;[14,17] both bases use the states generated by the hopping term in the Hamiltonian starting (usually) from the Néel state with a single hole.

The string idea is most useful in the Ising limit of the t-J model, when the hopping time scale is much shorter than the time scale for spin flips (which repair the damage to the Néel background done by the hole as it moves through the lattice). Recent numerical work has suggested, however, that the idea may prove useful in the Heisenberg limit: the spectral function (obtained from Lanczos calculations on 4×4 systems[18] and from diagonalization of the Hamiltonian in the hopping basis[17]) shows quasiparticle peaks that suggest stringlike excitations; also, the ground-state energy has power-law dependence on J/t, with an exponent about 10% larger than the value $\frac{2}{3}$ for strings.

The string and hopping bases have several advantages over exact-diagonalization studies (which have provided much of the current understanding of the t-J model). (i) Effectively infinite systems can be treated, eliminating finite-size effects (particularly unphysical interference effects due to periodic boundary conditions); little is known of the finite-size effects inherent to exact-diagonalization studies on small lattices (typically 4 × 4)—these effects could be important, in view of arguments for a long-range, dipolar spin distortion around the hole.[19,20] (ii)

All momenta can be studied (rather than just a few), and the effective (band) mass is easily obtained. (iii) The degeneracy of the momenta $(\pi,0)$ and $(\pi/2,\pi/2)$ found in 4×4 calculations is lifted in the larger systems (if enough states are included). (iv) The computational effort is concentrated on determining the structure in the immediate vicinity of the hole, rather than in attempting to find the structure of the entire system, the structure far from the hole being of no import for hole properties. (v) The infinite system allows the broken symmetry; a minor consequence is that the momenta (0,0) and (π,π) are degenerate (unlike finite-system results). On the other hand, the hopping term in the Hamiltonian is inefficient in generating spin flips (particularly flips far from the hole).

This paper uses the string and hopping bases to study a single hole in the t-J model and its variants. Section II describes the Lanczos procedure of Emery and Lin[11] for generating the string basis (and our implementation of it), and also the hopping basis.[14,17] Sections III, IV, and V present results for the $U=\infty$, t-J_z, and t-J models, respectively, and Sec. VI discusses the results.

II. STRING AND HOPPING BASES

The t-J Hamiltonian[2,21] is $H=H_t+H_z+H_\perp$ where

$$H_t=-t\sum_{<ij>\sigma}(\tilde{c}^\dagger_{i\sigma}\tilde{c}_{j\sigma}+\text{H.c.})\ , \tag{1}$$

$$H_z=J_z\sum_{<ij>}S^z_iS^z_j\ , \tag{2}$$

$$H_\perp=\frac{J_\perp}{2}\sum_{<ij>}(S^+_iS^-_j+S^-_iS^+_j)\ ; \tag{3}$$

in the t-J model proper, the coupling constants J_z and $J_\perp$ are identical and equal to $4t^2/U$. In the hopping term, $\tilde{c}_{i\sigma}=c_{i\sigma}(1-n_{i\bar{\sigma}})$ to prevent double occupancy. The above omits several terms: (i) three-site terms (studied by Trugman[17] and others) which arise in the canonical transformation from the Hubbard model to the t-J model; (ii) the term $-(J/4)\sum_{<ij>}n_in_j$ (which merely adjusts the zero of energy for the one-hole states we consider); and (iii) a direct next-nearest-neighbor hopping term (corresponding to oxygen-oxygen hopping in the $Cu\text{-}O_2$ planes). The parameters t and J are not known precisely, but it is believed that J is in the range $0.1t$ – $0.5t$, so that truncation of the canonical transformation at order t^2/U is likely adequate.

The starting state for the string basis is the Bloch state of a single hole in a Néel antiferromagnet; this state is defined to be the string state of length 0:

$$|0\rangle=\frac{1}{\sqrt{N}}\sum_i e^{i\mathbf{k}\cdot\mathbf{r}_i}\hat{T}_{\mathbf{r}_i}c_{0\downarrow}|\psi_{\text{Néel}}\rangle\ , \tag{4}$$

where N is the number of sites, $\hat{T}$ is the translation operator, $|\psi_{\text{Néel}}\rangle$ is the Néel state, and $c_{0\downarrow}$ destroys a down-spin electron at the origin. As the hole hops in the Néel background under the action of H_t, it leaves behind a string of misaligned spins. In the Lanczos procedure of Emery and Lin,[11] the string state $|n+1\rangle$ (of length $n+1$) is generated by applying H_t to the previous state $|n\rangle$:

$$|n+1\rangle=H_t|n\rangle-a_n|n\rangle-b_n|n-1\rangle\ . \tag{5}$$

H_t is tridiagonal in this basis, which is orthogonal and easily normalized. (For an infinite lattice, $a_n=0$ since the hole is on different sublattices in strings $|n\rangle$ and $|n+1\rangle$, but for finite lattices a_n can be nonzero.)

For calculational convenience we have not worked directly in the Lanczos basis but rather in a basis with no backward steps (no immediate returns to previous configurations). The states are generated as follows:

$$|\overline{n+1}\rangle=H_t|\overline{n}\rangle-\delta_n|\overline{n-1}\rangle\ , \tag{6}$$

where $\delta_n=-4t$ if $n=1$, and $-3t$ if $n>1$; the number of components of $|\overline{n}\rangle$ is $(4)3^{n-1}$ for $n\geq1$. The second (δ_n) term assures that only forward steps are taken; unlike the states $|n+1\rangle$ and $|n-1\rangle$, the states $|\overline{n+1}\rangle$ and $|\overline{n-1}\rangle$ have no trivial overlaps. Note that the loop graphs are included. The Lanczos basis vectors of Emery and Lin[11] are linear combinations of our $|\overline{n}\rangle$ states:

$$|n\rangle=\sum_{m=0}^{n}c_{nm}|\overline{m}\rangle\ ; \tag{7}$$

the coefficients c_{nm} can be determined recursively from Eq. (5).

The matrix elements of H_z and $H_\perp$ are easily found; the Appendix gives the leading matrix elements for the three terms in H. Note that H is not tridiagonal when the terms H_z and $H_\perp$ are included. In particular, H_z is not diagonal in the string basis; although each component of a given string state $|n\rangle$ is an eigenstate of H_z, the components have different Ising energies in general. Calculations can be done for any size lattice and we have results for lattices from 4×4 to 12×12. The latter is effectively infinite since we treat strings up to length 10; that is, we have determined the states $|\overline{n}\rangle$ for $n=0$ to $n=10$ inclusive. We have evaluated analytically the matrix elements of H_t and H_z for strings up to length 10 and the matrix elements of $H_\perp$ up to length 9.

For an infinite lattice, the matrix elements can be determined in the limit of very long strings. As Brinkman and Rice[9] have noted, for very long strings only the retracing paths (tree graphs) with no closed loops need be retained; other paths which also leave the spin background undisturbed are a negligibly small fraction of the total. In this retracing-path or tree approximation, the $(n+1)$th string has three times more components than the nth. These strings (which have no closed loops) asymptotically find themselves in a linear potential generated by the Ising term in the Hamiltonian. Finally, the spin-flip term connects $|n\rangle$ with $|n\pm2\rangle$. The limiting values (in the normalized Lanczos basis) are

$$\lim_{n\to\infty}\langle n|H_t|n\pm1\rangle=-\sqrt{3}\,t\ , \tag{8a}$$

$$\lim_{n\to\infty}\langle n|H_z|n\rangle=(n+1/2)J_z\ , \tag{8b}$$

$$\lim_{n\to\infty}\langle n|H_\perp|n\pm 2\rangle = D(\mathbf{Q})J_\perp/2. \tag{8c}$$

Equation (8a) is due to Brinkman and Rice,[9] and Eqs. (8b) and (8c) to Emery and Lin;[11] as in Ref. 11, $D(\mathbf{Q})$ is

$$D(\mathbf{Q}) = \cos Q_x + \cos Q_y + \cos Q_x \cos Q_y . \tag{9}$$

Because we are working with an antiferromagnetic backgound, the spatial periodicity is doubled, and we use the magnetic reciprocal-lattice vectors $Q_x = k_x + k_y$ and $Q_y = k_x - k_y$. We treated the first 11 ($n = 0 - 10$ inclusive) string states exactly, and then included the above asymptotic matrix elements up to length several hundred.

When the spin-flip terms in the Hamiltonian are not important, the ground-state wave function is composed of only a few short strings, for a wide range of parameters. When the spin flips are important, the ground-state energy (which we measure relative to the Néel state) is unreliable but quantities (such as the bandwidth, the effective masses, etc.) depending on energy differences are more accurately evaluated. But the string basis, which has s-wave symmetry, cannot treat properly the Heisenberg limit ($J_\perp = J_z$) of the t-J model. To treat this limit, it is important to relax the constraints on the components of a string state by using instead the hopping basis.[14,17]

The difference between the string and hopping bases is illustrated by considering the string basis to order 2. This has 17 different components (or spin configurations), but only three states: the Néel state with a single hole has one coefficient, the four components in order 1 a second, and the 12 components in order 2 a third. One sees that the string basis involves diagonalizing a smaller matrix, but has s-wave symmetry, and therefore treats improperly states with momentum different from (0,0), even in order 1. Further, there is no symmetry reason, even for momentum (0,0), for the 12 order-2 states to have the same coefficient. That is, the string basis places unreasonable constraints on the states, as noted previously.[17] In the hopping basis, on the other hand, the 17 spin configurations to order 2 are allowed to have different coefficients. Carried to completion, the hopping basis spans the Hilbert space for dimension $d \geq 2$ (but not for $d = 1$).

We generated the hopping basis by applying the hopping term H_t repeatedly to the Néel state with a single hole. The ground state was found by diagonalizing the full Hamiltonian in the basis of states generated by up to eight hops, a total of 9786 distinct states; previous work used smaller bases. The method is a variant of that of Trugman,[14,17] who included also states generated by the three-site hopping term, and has been used also by Inoue and Maekawa.[22]

Since the hopping basis treats each spin configuration as independent, it can treat the Heisenberg limit and states of symmetry other than s wave; on the other hand, it is limited to a smaller number of hops (eight in our case versus ten for the string basis), and it cannot be extended to infinite order by the tree approximation. The two methods are competitive for the t-J_z model at moderate values of $J_z/t(> 0.1)$; the string method fails for the t-J model (with $J_\perp = J_z$), whereas the hopping basis appears to give good results for $J > 0.1t$ (even for $J > t$, which is outside both the physical region and the region of validity of the model).

A Green function is defined by

$$G(\mathbf{k},\omega) = \frac{1}{N}\sum_{i,j} e^{i\mathbf{k}\cdot(\mathbf{r}_i-\mathbf{r}_j)} G_{ij}(\omega) \tag{10}$$

with

$$G_{ij}(\omega) = \langle\tilde{i}|(\omega - H)^{-1}|\tilde{j}\rangle . \tag{11}$$

Here $|\tilde{i}\rangle = \hat{T}_{\mathbf{r}_i} c_{0\downarrow}|\psi_{\text{Néel}}\rangle$ represents a hole at site i in an otherwise Néel background. As defined, the function is useful only for the J=0 and t-J_z models; to treat the t-J model, we would require the ground state of the Heisenberg model (otherwise the spectrum would be dominated by the excitations of the antiferromagnet, not those of the hole). Since the Taylor series in H/ω converges only for $|\omega| > zt$ (z is the coordination number of the lattice), we use instead a continued-fraction representation. The Green function is split into dispersionless and dispersive contributions:

$$G(\mathbf{k},\omega) = G_{ii}(\omega) + \sum_{\delta} e^{i\mathbf{k}\cdot\delta} G_\delta(\omega) , \tag{12}$$

where $\delta = \mathbf{r}_i - \mathbf{r}_j$. The spectral-density function is

$$A(\mathbf{k},\omega) = -\frac{1}{\pi}\,\text{Im}\, G(\mathbf{k},\omega + i\epsilon) ; \tag{13}$$

in principle $\epsilon = 0^+$, but nonzero ϵ is useful in plotting results.

III. $U = \infty$ MODEL

This section studies the properties of a single hole in the t-J model at $J = 0$ ($U = \infty$). Of course the ground state of a single hole at $U = \infty$ is ferromagnetic[23] (the momentum is $\mathbf{k} = (\pi, \pi)$ in a 4×4 Lanczos calculation). Our study of a hole hopping in an antiferromagnetic background is intended to lay a basis for understanding the t-J_z and t-J models of Secs. IV and V.

The $J = 0$ limit of the t-J model was examined by Brinkman and Rice,[9] who enumerated paths and noted the existence of closed paths which restore the Néel background and return the hole to its original position; the shortest such loop runs three times around a plaquette. In the tree approximation[9] (which sums the retracing paths to all orders), the Green function is dispersionless, and the band mass infinite. The site-diagonal term G_{ii} in Eq. (12) has been evaluated[9,24] using a moment expansion and also analytically including only retracing paths. The bandwidth (a misleading term since quasiparticles do not exist in the tree approximation, and the band mass is infinite) is approximately $4\sqrt{3}\,t$ (versus $8t$ for a ferromagnetic background); Brinkman and Rice[9] argued that exponentially small band tails continue to $\pm 4t$.

Subsequently, Trugman[14] pointed out paths which also restore the Néel background, but displace the hole by $\sqrt{2}a$ or $2a$ to a point on the same sublattice; the shortest

such path runs $1\frac{1}{2}$ times around a plaquette of four sites. These paths produce a momentum dependence and a finite band mass. The leading $\mathbf{k}$-dependent contribution to $G(\mathbf{k},\omega)$ is[14] $(4/\omega)(t/\omega)^6(\cos Q_x + \cos Q_y)$, which is of order t^6; the hole is displaced $\sqrt{2}a$ by the six hops. These paths and many others which restore the Néel background are included in our analysis, which treats strings up to length 10 exactly (terms of order t^{20} in G), and sums the remainder in the tree approximation.

We have used both the string and hopping bases, but present results only for the former (which gives the lower energy). Figure 1(a) plots the spectral function $A(\mathbf{k},\omega)$ at the energy minimum $\mathbf{k} = (0,0)$, and, for comparison, the spectral function A in the full tree approximation.[9] For $J = 0$, A is even in ω: the gauge transformation $c_{i\sigma} \rightarrow \exp(i\mathbf{Q}\cdot\mathbf{r}_i)c_{i\sigma}$ carries H into $-H$; since $\mathbf{Q}$ is a magnetic reciprocal-lattice vector in the Néel backgrounds we consider, we have $A(\mathbf{k}+\mathbf{Q},\omega) = A(\mathbf{k},-\omega)$ and hence the even symmetry for $J = 0$. Qualitatively the spectral function is similar to Fig. 5(g) of Dagotto *et al.*;[25] there is a peak at the band edge, and states near $\omega = 0$ are depleted. The spectral function for other values of $\mathbf{k}$ lacks the peaks at the band edges. The lower band edge decreases only slightly as the accuracy of the calculation is improved, from $-2\sqrt{3}\,t \simeq -3.46t$ in the tree approximation[9] to $\simeq -3.49t$ when strings up to length 10 are treated exactly (and the tree approximation is used for the remainder). The structure in the region $1 < |\omega|/t < 3$ changes with the order of the approximation (as longer strings are treated exactly), but the peaks at the band edges are stable. We found no evidence for a ferromagnetic region near the hole: the nearest-neighbor $< S_i^z S_j^z >$ correlation function is antiferromagnetic near the hole, but half the Néel value.

Figure 1(b) shows the real and imaginary parts of the self-energy. The spectral function has sharp peaks at the lower and upper edges, but there are no quasiparticles since the imaginary part of the self-energy is large where $\omega = \mathrm{Re}\Sigma$. For J_z and $J_\perp$ different from zero, the peak at the band edge develops into a long-lived quasiparticle (but at a different momentum); see Secs. IV and V.

The dispersion relation for the lowest band is flat over the entire Brillouin zone, except close to the minimum at $\mathbf{k} = (0,0)$; at this point, the band mass m^* (defined by

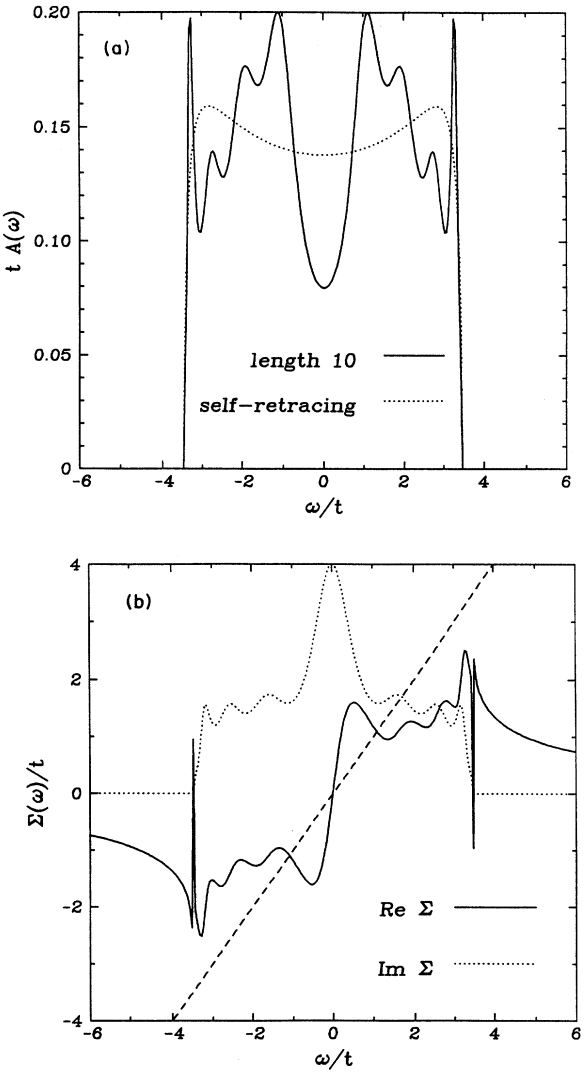

FIG. 1. Spectral function and self-energy for the $U = \infty$ model at k = (0, 0); strings up to length 10 are treated exactly, and the remainder are summed to infinite order in the tree approximation. (a) Comparison of the spectral functions in our string approximation (solid line) and in the tree approximation (Ref. 9) (dotted line). The functions are unbroadened [$\epsilon = 0^+$ in Eq. (13)]. (b) Real and imaginary parts of the self-energy; the dashed line is $\mathrm{Re}\Sigma = \omega$.

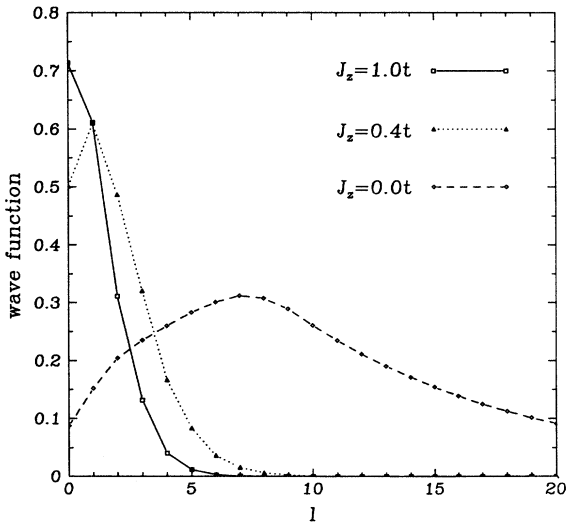

FIG. 2. Amplitude of the wave function in the string basis for $J_z = 0, 0.4t$, and t, at momentum $\mathbf{k} = (0,0)$. For $J_z = 0$, retracing paths are included (as described in the caption to Fig. 1); convergence was not obtained even at string length 10, and the result for this value of J_z has at best qualitative validity.

$1/m^*_{ij} = \partial^2 E/\partial k_i \partial k_j$) is isotropic and close to twice the bare mass $m = 1/(2t)$: $m^* = 2.087m$.

Inclusion of the Trugman paths makes a major modification to the wave function. If only the tree graphs (retracing paths) are included, the average string length diverges as longer walks are taken. The wave function is extended also in the string basis, when the maximum string length is 5 or less; but there is an abrupt transition to an apparently localized wave function at string length 6, when the wave function includes the shortest Trugman path. Beyond length 6, the average string length remains finite. Figure 2 shows the amplitude of the wave function (which is exponential at large string lengths). The plot is qualitative only (convergence is not obtained even at string length 10); we caution that the validity of the string basis is doubtful at such large lengths.

IV. t-J_z MODEL

The Ising term H_z in the Hamiltonian acts to confine the hole,[8,10] and the string basis can be truncated at reasonable size even when J_z is small, the truncation becoming more accurate with increasing J_z. The wave functions are plotted in Fig. 2; for $J_z < 0.1t$, the wave function depends significantly on the order of the approximation (the number of string states treated exactly), but we expect our string calculation (which includes all loop processes to order t^{20}) to be reasonably accurate for $J_z > 0.1t$. The analytical calculation of Johnson *et al.*[15] includes only the leading loop path (of order t^6) and is likely good down to $J_z = 0.2t$. But our string calculation still misses the ferromagnetic tendency for very small J_z.

Figure 3 plots the ground-state energy as a function of J_z, and also the second-order perturbation theory result $-8t^2/3J_z$ and the following fit in the range $0.1t < J_z < 0.8t$ (with the exponent constrained to the continuum-theory value[10,26]): $(E+J_z)/t = -3.580+2.860(J_z/t)^{2/3}$. [The energy offset of J_z/t is due to our definition of the reference state as $|0\rangle$ (the Néel state with a hole), rather than the Néel state as in other work.[10,26]] The above coefficients are comparable with the values (−3.464,2.74) of Shraiman and Siggia[10] (whose string basis included only retracing paths) and with the Monte Carlo values[26] (−3.63,2.93). As seen from Table I, the ground-state energies obtained by three different methods, Monte Carlo[26] (adjusted for the different energy zero), string basis, and hopping basis, agree well for $J_z \geq 0.2t$; 4×4 Lanczos results (from independent calculations) give much the same results. The hopping energies are slightly better for $J_z > 0.17t$ (approximately), when the average string length is small (because of the greater freedom in the coefficients), but the string energies are better for $J_z < 0.17t$ because the string calculation includes more hops and uses the tree approximation to extend the results. For $J_z < 0.1t$, the 8×8 Monte Carlo values suffer from finite-size effects (see Fig. 2 of Barnes *et al.*[26]); the departure from $(J_z/t)^{2/3}$ behavior in this region is not a ferromagnetic tendency — the ferromagnetic polaron, with energy $E \simeq -4t + 8.5(J_z t)^{1/2}$, starts to form at[10] $J_z = 5 \times 10^{-3}t$.

For all J_z, the energy minimum is at $\mathbf{k}=(0,0)$ and the maximum at $\mathbf{k}=(\pi,0)$. Figure 4 plots the dispersion relation over the Brillouin zone; the corresponding density of states shows a logarithmic singularity in the middle of the band due to saddle points at the Δ points $(\pm\pi/2,\pm\pi/2)$. These results are similar to those for the ferromagnet, but rotated by $\pi/4$ to the magnetic Brillouin zone; perturbation theory in the large-J_z limit gives the leading momentum-dependent term as

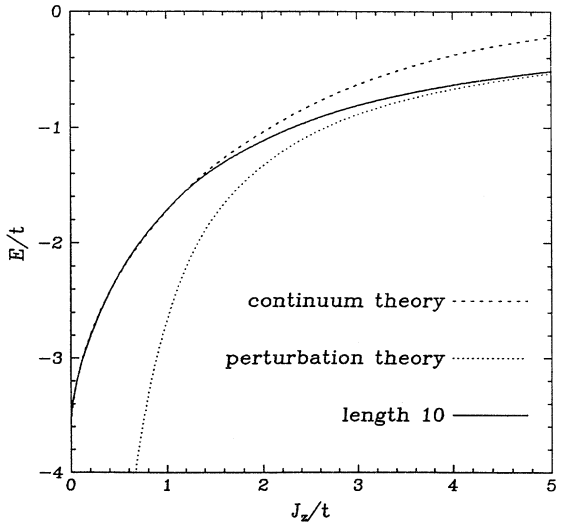

FIG. 3. Ground-state energy of the t-J_z model compared to large-J_z perturbation theory and the continuum theory (Ref. 10).

TABLE I. Comparison of Monte Carlo (Ref. 26), string-basis and hopping-basis results for the ground-state energy of the t-J_z model. The Monte Carlo systems were of size 8×8 for $J_z/t < 1.5$ and 6×6 for $J_z/t \geq 1.5$; energies without error estimates have undetermined systematic errors. The last column gives the average string length $< l >$ (as determined by the string method).

J_z/t	Monte Carlo	String basis	Hopping basis	$< l >$
0		−3.4940	−3.3940	8.56
0.01	≈ −3.71	−3.4280	−3.3573	6.30
0.02	≈ −3.47	−3.3742	−3.3216	5.40
0.05	≈ −3.29	−3.2429	−3.2205	3.91
0.1	≈ −3.10	−3.0741	−3.0694	2.80
0.2	−2.830 ± 0.007	−2.8152	−2.8169	1.95
0.4	−2.444 ± 0.008	−2.4298	−2.4315	1.31
0.6	−2.142 ± 0.008	−2.1380	−2.1391	0.98
0.8	−1.903 ± 0.011	−1.9053	−1.9060	0.77
1.0	−1.706 ± 0.006	−1.7144	−1.7148	0.63
1.5	−1.359 ± 0.010	−1.3596	−1.3597	0.40
2.0	−1.113 ± 0.004	−1.1164	−1.1164	0.28
2.5	−0.946 ± 0.006	−0.9414	−0.9414	0.20
3.0	−0.811 ± 0.002	−0.8107	−0.8107	0.15

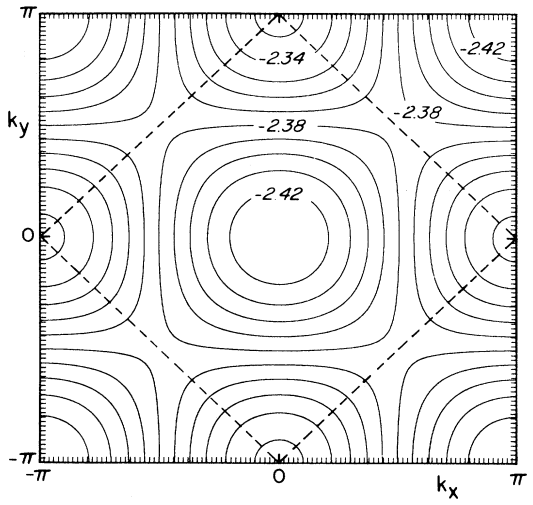

FIG. 4. Contour plot (interval 0.01) of the dispersion relation for the lowest quasiparticle in the t-J_z model at $J_z = 0.4t$; $-\pi \leq k_x, k_y \leq \pi$. The minimum is at the origin and the maximum at $(\pi, 0)$; the saddle point is at $(\pm\pi/2, \pm\pi/2)$, on the magnetic zone boundary (dashed lines).

$\propto (t^6/J_z^5)(\cos Q_x + \cos Q_y)$, due to the Trugman paths, which is like the ferromagnetic result with $\mathbf{k} \rightarrow \mathbf{Q}$.

Figure 5 compares the bandwidth $W = E(\pi, 0) - E(0, 0)$ in our string calculation (the hopping-basis bandwidth is about 1% smaller) with the exact (Lanczos) bandwidth for a 4 × 4 system. The results agree qualitatively except at very small J_z (where the string results are invalid; but, in contrast to many calculations, the string bandwidth does not vanish at $J_z = 0$). The string results agree reasonably well with those of Johnson *et al.*,[15] who have, however, questioned the peak in the bandwidth (the peak appears to be real in our calculations). The large-J_z fit to the bandwidth has the form[15] $W = A\exp[-B(J_z/t)^{1/2}]$, which arises naturally from tunneling through the triangular barrier [see Fig. 3(b) of Trugman[14]] generated by the Ising term H_z as the hole loops $1\frac{1}{2}$ times around a plaquette. In rough agreement with Johnson *et al.*,[15] we find A=3.158 and

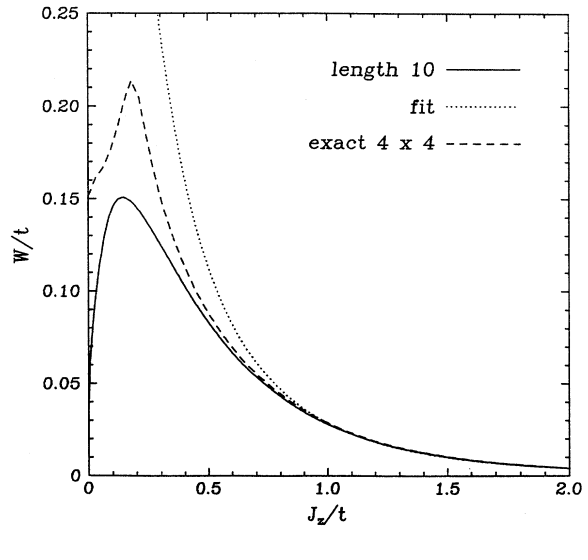

FIG. 5. Bandwidth $W = E(\pi, 0) - E(0, 0)$ of the t-J_z model. The string basis (solid line) gives results in reasonable agreement with those of Johnson *et al.* (Ref. 15), but there are differences at small J_z. The exact-diagonalization result for a 4 × 4 system (dashed line) also shows a peak. The dotted line is a fit to the large-J_z result (Ref. 15) for tunneling through a triangular barrier.

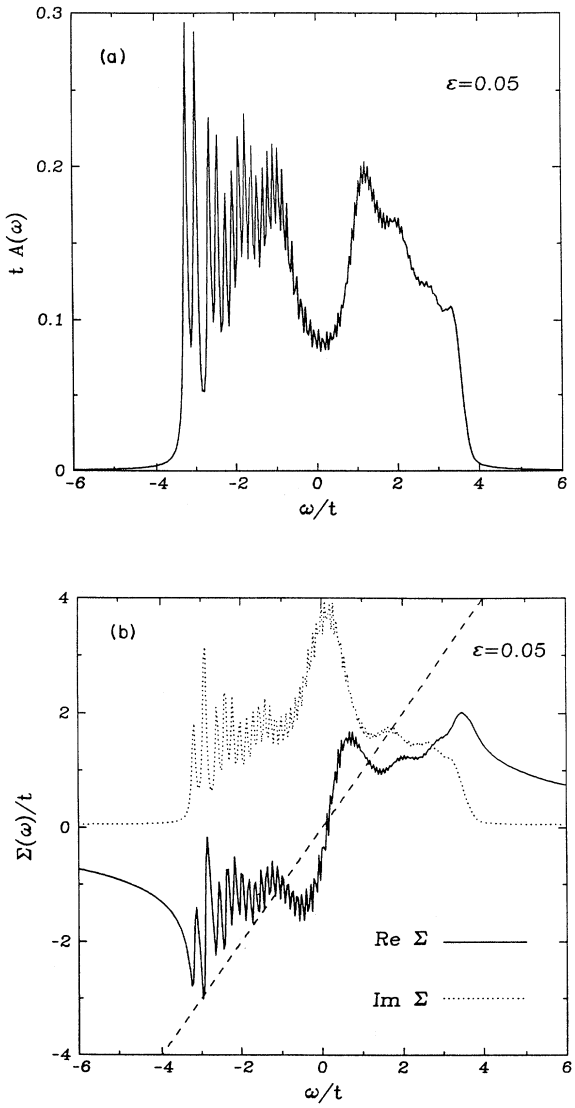

FIG. 6. Spectral function (a) and self-energy (b) for the t-J_z model at J_z=0.05t and $\mathbf{k} = (0, 0)$. Strings up to length 10 are treated exactly, and strings of length 11 – 250 in the tree approximation; the functions are unchanged to higher order in the tree approximation — that is, the fine structure is not due to truncation at length 250.

B=4.710. The effective mass at the $\mathbf{k} = (0,0)$ minimum varies little with J_z in the physical region of parameter space; for example, m^*=2.130m at J_z=0.4t, and in general $m^*/m \approx$ 1–2. The hopping basis gives a slightly larger mass, m^*=2.242m at J_z=0.4t.

Figures 6 and 7 plot the spectral function and the self-energy for J_z=0.05t and J_z=0.4t, respectively; also plotted for J_z=0.4t is the spectral function obtained using the hopping basis. The string basis captures the low-energy behavior and also the total spectral width, but the high-energy behavior is flatter in the hopping basis. As predicted by Kane, Lee, and Read,[27] and found in other numerical work,[18] there is a clear quasiparticle peak at the bottom of the band (at J_z=0.4t); the peak is reasonably well developed even at J_z=0.05t. The weight of this peak scales like J_z up to J_z=0.1t; in agreement with the continuum results, the separation between the low-energy poles behaves as $(J_z/t)^{2/3}$.

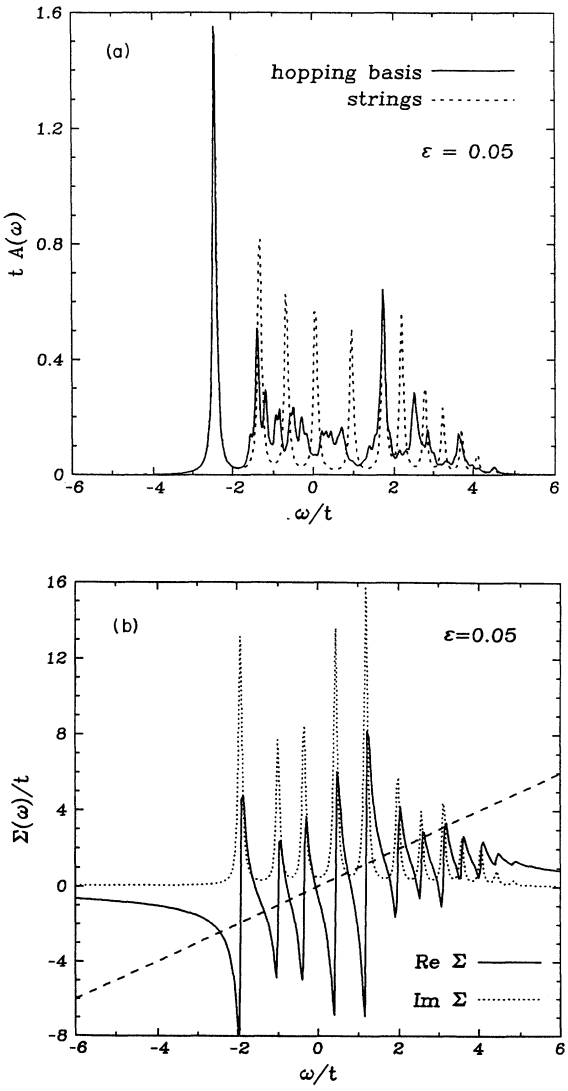

FIG. 7. (a) Spectral functions (string and hopping bases) and (b) self-energy (string basis) for the t-J_z model at J_z=0.4t and $\mathbf{k} = (0,0)$; the approximation is described in the caption to Fig. 6. Note that the lifetime is large for the lowest quasiparticle.

We have also examined the spectral function obtained by exact diagonalization for a 4 × 4 system (where the string self-interaction effects begin at strings of length four) and compared it with the string result. At $J_z = 0.4t$ and $\mathbf{k} = (0,0)$, the properties of the lowest pole are the same, and the two results have the same total spectral width, but the structure at intermediate energies is quite different: the 4 × 4 result has a gap near $\omega = t$, while the string result has weight in this region. For $J_z > t$, where the strings are short, the 4 × 4 and string spectra are almost identical at all energies; examination of the self-energy shows that the string quasiparticles are well defined.

For nonzero J_z, the hole forms a region of disrupted Néel order around itself as it gains kinetic energy by hopping. In the frame moving with the hole, the nearest-neighbor correlation function $< S_i^z S_j^z >$ close to the hole is reduced to 60% of the Néel value (at $J_z = 0.4t$). The average string length, defined as $< l >= \sum_l l\langle l|l\rangle$, is a measure of the polaron size; our results are fitted by $< l >= 1.84(J_z/t)^{-1/3} - 1.18$ for $0.05 \leq J_z/t \leq 8$ (the exponent $-1/3$ is the continuum-theory value); like Barnes *et al.*,[26] who determined the number of "anti-Néel spins," we find a large negative contribution independent of J_z.

V. t-J MODEL

The spin-flip terms in $H_\perp$ repair the damage done as the hole moves through the lattice. In the t-J_z model ($J_\perp$=0), the energy minimum is at $\mathbf{k} = (0,0)$, but a level crossing occurs as $J_\perp$ is increased, and the minimum shifts to $\mathbf{k} = (\pi/2, \pi/2)$ (the center of the magnetic zone face), in agreement with previous work.[14,19,22,15] The level crossing (studied in detail by Johnson *et al.*[15]) is easily understood: at lowest order,[20,28] the effect of $H_\perp$ on the dispersion is proportional to $J_\perp D(\mathbf{Q})$ which is a minimum on the magnetic zone boundary ($k_x \pm k_y = \pm\pi$); the degeneracy is lifted in higher order.

In view of the reservations expressed in Sec. II, the string basis is not the method of choice for examining the t-J model, particularly since the ground state has nonzero momentum for parameter values of physical interest. Since the hopping term in the Hamiltonian is inefficient in generating spin flips, the string basis (and for that matter also the hopping basis) appears to require both $J_\perp \ll t$ and $J_\perp \ll J_z$. Our numerical work suggests, however, that the string basis is useful in the region $J_\perp \leq 0.1t$ and $J_\perp \leq \frac{1}{4}J_z$. In the following, we present results obtained using both bases; the hopping basis appears to treat accurately the Heisenberg case $J_\perp = J_z$ in the range of physical interest ($0.1t < J < 0.5t$) and beyond.

The string results for the bandwidth W compare well with other results[15] for $J_z < t$ and $\alpha = \frac{1}{4}$; here $\alpha = J_\perp/J_z$. For larger J_z, and the same α, the string results are poor; the bandwidth decreases linearly and eventually vanishes, instead of decreasing as[15] $1/J$. The behavior of the string result is understood as follows. The ground-

state wave function and energy to second order in $1/J_z$ (obtained by diagonalizing H in the basis $|0\rangle$, $|1\rangle$, and $|2\rangle$ for $J_z \gg t, J_\perp$) are

$$|gs\rangle = |0\rangle + \frac{4t}{3J_z}|1\rangle + \left(\frac{8\sqrt{3}}{15}\frac{t^2}{J_z^2} - \frac{2D(\mathbf{Q})J_\perp}{5\sqrt{3}J_z}\right)|2\rangle \ , \tag{14}$$

$$E = -\frac{8t^2}{3J_z} - \frac{2}{15}D^2(\mathbf{Q})\frac{J_\perp^2}{J_z} + \frac{16}{15}D(\mathbf{Q})\frac{t^2 J_\perp}{J_z^2} \ . \tag{15}$$

The second term on the right-hand side of Eq. (15) is responsible for the incorrect behavior when $J_z > t$, and $\alpha = \frac{1}{4}$. The hopping basis corrects this unphysical behavior; for large J, the bandwidth falls off as t^2/J in agreement with perturbation theory[20] and in contrast to 4×4 Lanczos results (see the discussion in Ref. 29).

Figure 8 gives a contour plot of the dispersion relation for $J_z = 0.4t$ and $J_\perp = 0.1t$; the minimum is at $\mathbf{k} = (\pi/2, \pi/2)$ for these values. Figure 9 plots the energy along the high-symmetry directions for $J_z = 0.4t$ and three values of α. The density of states for $J_z = 0.4t$ and $J_\perp = 0.1t$ is shown in Fig. 10; in addition to the logarithmic singularity (from the saddle points) and the discontinuities at the lower and upper energies, there is a discontinuity due to the local maximum at $(\pi, 0)$ (seen clearly in Fig. 9). With increasing α, the region around $(\pi, 0)$ becomes flatter, the discontinuity in the density of states disappears, and the logarithmic singularity moves from the center of the band (for the t-J_z model) toward the discontinuity at the lower band edge. That is, the density of states seems to be evolving to a form similar to that for the lower band in the commensurate spin-density wave at zero doping in the Hubbard model. These results are similar to other numerical work.[30] The average string length (for fixed α) behaves as $J_z^{-1/3}$, but over a much smaller region than in the t-J_z model. Chen and Schüttler[31] have argued for a bandwidth W [defined as $W = E(\pi/2, \pi/2) - E(0,0)$] behaving as $W \propto \exp(t/J)^\beta$ due to polaron formation around the hole. For fixed $\alpha =$

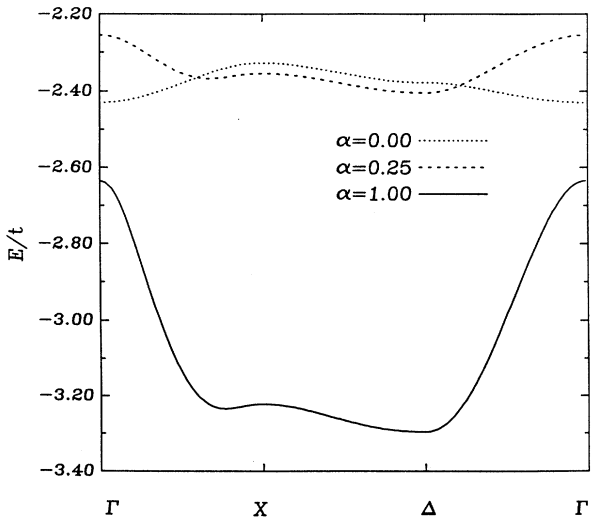

FIG. 9. Dispersion relation of the t-J model for J_z=0.4t and three values of the transverse coupling $J_\perp = \alpha J_z$; Γ, X, and Δ are k=(0,0), $(\pi, 0)$, and $(\pi/2, \pi/2)$, respectively. Note the relative maximum at the X point for $J_\perp = 0.25J_z$ and $J_\perp = J_z$. Only relative values of the energy are significant; in particular, the $J_\perp = 0$ and $J_\perp = 0.25J_z$ results are from string calculations, while the Heisenberg result ($J_\perp = J_z$) was obtained using the hopping basis (hence the large energy drop).

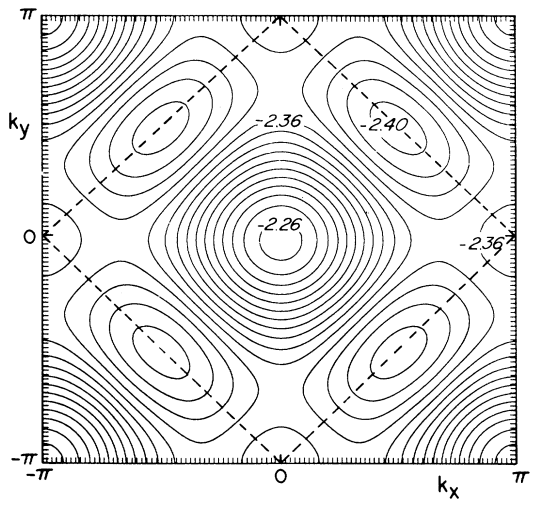

FIG. 8. Contour plot (interval 0.01) of the dispersion relation for the lowest quasiparticle in the t-J model at $J_z = 0.4t$ and $J_\perp = 0.1t$; $-\pi \le k_x, k_y \le \pi$. The minimum is at the center of the magnetic zone face, and the maximum at the origin; there is a relative maximum at $(\pi, 0)$.

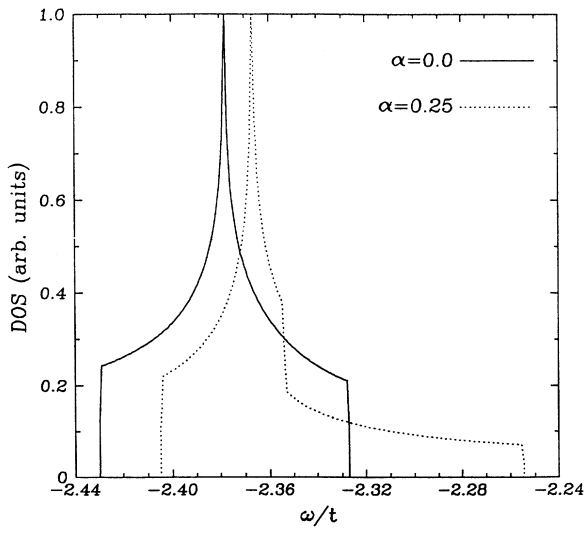

FIG. 10. Density of states (in arbitrary units) for the t-J model with J_z=0.4t, and $J_\perp$= 0 and 0.1t; the discontinuity at $\omega/t \simeq -2.35$ is due to the local maximum at the X point — see Fig. 9.

$\frac{1}{4}$, we find that $\ln W$ is linear in t/J_z for $0.2 < J_z/t < 0.6$, in weak confirmation of this idea. The results of this paragraph were obtained using the string basis.

The band mass around the $(\pi/2, \pi/2)$ minimum is anisotropic. For example, at $J_z=0.4t$, $J_\perp=0.1t$ the band masses parallel and perpendicular to the zone face are $m_\parallel=2.125m$ and $m_\perp=0.618m$. At $J_z=J_\perp=0.4t$ the anisotropy is even greater: $m_\parallel=20.4m$ and $m_\perp=2.10m$. A heavy mass along the zone boundary agrees with previous results obtained by fitting to Lanczos calculations on an 18-site cluster,[20] and by use of the hopping basis.[17,22] Our masses are heavier than those of Elser *et al.*,[20] but comparable to those of Trugman.[17]

We have also examined the spectral function, but do not present detailed results for the reason given in Sec. II. As noted by Trugman,[17] the hopping basis accurately captures the low-energy behavior; the structure at higher energy is sensitive to the number of hops included, becoming smoother as more states are included.

The string method can be applied also in one dimension (where, however, the string basis does not span the Hilbert space). All matrix elements can be evaluated exactly; the Green function for a hole moving in a Néel background in the limit $J_\perp \ll t$ is

$$G(k,\omega) = \{ (J_z/2 + J_\perp \cos 2k) + \\ +[(\omega - J_z/2 - J_\perp \cos 2k)^2 - 4t^2]^{1/2}\}^{-1} .$$

This generalizes a result of von Szczepanski *et al.*[28] (who treated the case $J_z = 0$).

VI. DISCUSSION

For the $U = \infty$ model (with an antiferromagnetic background), the string method (which includes Trugman paths to many orders) gives apparently localized wave functions (in contrast to the extended wave functions predicted by the tree approximation). But the imaginary part $\mathrm{Im}\Sigma$ of the self-energy is large when $\mathrm{Re}\Sigma = \omega$, and there are no quasiparticles.

For the t-J_z model, the string and hopping results appear accurate for $J_z > 0.1t$; both methods give ground-state energies in excellent agreement with Monte Carlo values. Both the string and hopping methods fail when the ferromagnetic polaron begins to form around the hole, when[10] $J_z/t \approx 5 \times 10^{-3}$; at $J_z = 0$, even strings up to length 10 do not capture the polaron.

For the t-J model, which is the model of interest for the high-T_c materials, the string method is less useful (because it imposes unreasonable constraints on the basis). The validity of the string method is likely restricted to $J_\perp \leq 0.1t$, and so the Heisenberg limit $J_\perp = J_z$ for physically interesting values of the parameters cannot be discussed. But in the region $J_\perp \leq 0.1t$, the string results agree with other results: the ground-state momentum is at the center of the zone edge, the bandwidth is given accurately, etc. On the other hand, the hopping basis seems to give accurate results for all $J > 0.1t$, even though constructing a basis from H_t alone is questionable when t and $J_\perp$ are of the same order. Spin flips far from the hole (these are not easily generated by H_t), though

TABLE II. Leading matrix elements in the $|\overline{n}\rangle$ basis.

n,m	$\langle\overline{n}\|H_t\|\overline{m}\rangle/(-t)$	$\langle\overline{n}\|H_z\|\overline{m}\rangle/J_z$	$\langle\overline{n}\|H_\perp\|\overline{m}\rangle/(J_\perp/2)$
0,0	1	0	0
1,1	4	6	0
2,2	12	30	0
2,0	0	0	$8\gamma_Q^{(1)} + 4\gamma_Q^{(2)}$
3,1	0	0	$8 + 24\gamma_Q^{(1)} + 12\gamma_Q^{(2)}$
3,3	$36 + 8\gamma_Q^{(1)}$	$122 + 24\gamma_Q^{(1)}$	0
4,0	0	0	8
4,2	$8\gamma_Q^{(1)}$	$20\gamma_Q^{(1)}$	$32 + 64\gamma_Q^{(1)} + 36\gamma_Q^{(2)}$
4,4	$108 + 16\gamma_Q^{(1)}$	$446 + 56\gamma_Q^{(1)}$	$48\gamma_Q^{(1)} + 48\gamma_Q^{(2)} + 32\gamma_Q^{(3)} + 32\gamma_Q^{(4)}$
5,1	$8\gamma_Q^{(1)}$	$12\gamma_Q^{(1)}$	16
5,3	$16\gamma_Q^{(1)}$	$56\gamma_Q^{(1)}$	$136 + 240\gamma_Q^{(1)} + 148\gamma_Q^{(2)} + 32\gamma_Q^{(3)} + 32\gamma_Q^{(4)}$
5,5	$324 + 64\gamma_Q^{(1)} + 32\gamma_Q^{(2)}$	$1578 + 272\gamma_Q^{(1)} + 112\gamma_Q^{(2)}$	$32 + 256\gamma_Q^{(1)} + 112\gamma_Q^{(2)} + 64\gamma_Q^{(3)} + 64\gamma_Q^{(4)}$

vital for the ground-state energy, appear to be unimportant for the hole properties; the suggestion is that the hole is well confined (except for small J), making only short excursions, and that the spin flips generated by H_t are sufficient to describe the hole properties.

ACKNOWLEDGMENTS

We thank P. Voruganti, A. Griffin, and T. Barnes for interesting and instructive discussions, and V. J. Emery and H. Q. Lin for describing to us their Lanczos procedure for generating the string basis. This research was supported by the Natural Sciences and Engineering Research Council of Canada.

APPENDIX

Table II gives the leading nonzero matrix elements (up to six strings) in the $|\overline{n}\rangle$ basis for the three terms of H in Eqs. (1), (2), and (3); only elements with $n \geq m$ are given since the matrix is symmetric. The leading 16 elements ($m, n = 0 - 3$) agree with those given by Emery.[11] Note that the $|\overline{n}\rangle$ basis, defined by Eq. (6), is not normalized. The matrix elements in the Lanczos basis $|n\rangle$ are constructed using Eq. (7). The results reported in the text were obtained with the full 11×11 matrix for H_t and H_z, and the 10×10 matrix for $H_\perp$; the asymptotic relations of Eq. (8) were used for $\langle n|H_t|m\rangle$ and $\langle n|H_z|m\rangle$ (n or $m > 10$) and $\langle n|H_\perp|m\rangle$ (n or $m > 9$). The cubic harmonics (normalized so that $|\gamma_Q| \leq 1$) are defined by

$$\gamma_Q^{(1)} = (\cos Q_x + \cos Q_y)/2 \ ,$$

$$\gamma_Q^{(2)} = \cos Q_x \cos Q_y \ ,$$

$$\gamma_Q^{(3)} = (\cos 2Q_x + \cos 2Q_y)/2 \ ,$$

$$\gamma_Q^{(4)} = (\cos 2Q_x \cos Q_y + \cos Q_x \cos 2Q_y)/2 \ .$$

[1] J. G. Bednorz and K. A. Müller, Z. Phys. B **64**, 189 (1986).
[2] P. W. Anderson, Science **235**, 1196 (1987).
[3] P. W. Anderson (unpublished).
[4] J. Hubbard, Proc. R. Soc. London, Ser. A **276**, 238 (1963).
[5] R. J. Birgeneau *et al.*, Phys. Rev. B **38**, 6614 (1988).
[6] S. Liang, Phys. Rev. B **42**, 6555 (1990).
[7] T. Barnes, Int. J. Mod. Phys. C **2**, 659 (1991).
[8] L. N. Bulaevskii, É. L. Nagaev, and D. I. Khomskiĭ, Zh. Eksp. Teor. Fiz. **54**, 1562 (1968) [Sov. Phys. JETP **27**, 836 (1968)].
[9] W. F. Brinkman and T. M. Rice, Phys. Rev. B **2**, 1324 (1970).
[10] B. I. Shraiman and E. D. Siggia, Phys. Rev. Lett. **60**, 740 (1988).
[11] V. J. Emery and H. Q. Lin, Bull. Am. Phys. Soc. **34**, 1035 (1988) and (unpublished). Emery has described the Lanczos procedure for generating the string basis.
[12] B. D. Simons and J. M. F. Gunn, Phys. Rev. B **41**, 7019 (1990); J. M. F. Gunn and B. D. Simons, *ibid.* **42**, 4370 (1990).
[13] R. Eder and K. W. Becker, Z. Phys. B **78**, 219 (1990).
[14] S. A. Trugman, Phys. Rev. B **37**, 1597 (1988).
[15] M. D. Johnson, C. Gros, and K. J. v. Szczepanski, Phys. Rev. B **43**, 11 207 (1991).
[16] N. Kumar, Phys. Rev. B **42**, 6138 (1990).
[17] S. A. Trugman, Phys. Rev. B **41**, 892 (1990).
[18] E. Dagotto, A. Moreo, R. Joynt, S. Bacci, and E. Gagliano, Phys. Rev. B **41**, 2585 (1990).
[19] B. I. Shraiman and E. D. Siggia, Phys. Rev. Lett. **61**, 467 (1988).
[20] V. Elser, D. A. Huse, B. I. Shraiman, and E. D. Siggia, Phys. Rev. B **41**, 6715 (1990).
[21] F. C. Zhang and T. M. Rice, Phys. Rev. B **37**, 3759 (1988).
[22] J. Inoue and S. Maekawa, J. Phys. Soc. Jpn. **59**, 2110 (1990).
[23] Y. Nagaoka, Phys. Rev. **147**, 392 (1966).
[24] Y. S. Yang, C. J. Thompson, and A. J. Guttmann, Phys. Rev. B **42**, 8431 (1990).
[25] E. Dagotto, R. Joynt, A. Moreo, S. Bacci, and E. Gagliano, Phys. Rev. B **41**, 9049 (1990).
[26] T. Barnes, E. Dagotto, A. Moreo, and E. S. Swanson, Phys. Rev. B **40**, 10 977 (1989).
[27] C. L. Kane, P. A. Lee, and N. Read, Phys. Rev. B **39**, 6880 (1989).
[28] K. J. von Szczepanski, P. Horsch, W. Stephan, and M. Ziegler, Phys. Rev. B **41**, 2017 (1990).
[29] T. Barnes, A. E. Jacobs, M. D. Kovarik, and W. G. Macready, Phys. Rev. B (to be published).
[30] G. Vignale and M. R. Hedayati, Phys. Rev. B **42**, 786 (1990).
[31] C.-X. Chen and H.-B. Schüttler, Phys. Rev. B **41**, 8702 (1990).